Purdue University
Purdue e-Pubs

International Refrigeration and Air Conditioning Conference

School of Mechanical Engineering

2018

Frost Porosity Measurement Using Capacitive Sensor

Yuchen Shen
University of Illinois at Urbana-Champaign, United States of America, yshen51@illinois.edu

Yuheng Zhang
University of Illinois at Urbana-Champaign, United States of America, yuhengzhang1990@gmail.com

Xiaofei Wang
University of illinois at urbana champaign, United States of America, wangxf@illinois.edu

Real-Time Frost Porosity (Density) Measurement Using Capacitive Sensor

Yuchen Shen[1], Yuheng Zhang[1], Xiaofei Wang[1]*

[1]University of Illinois at Urbana-Champaign
Department of Mechanical Science and Engineering,
1206 West Green Street, Urbana, IL 61801, USA

* Corresponding Author Email: wangxf@illinois.edu

ABSTRACT

In this work, a capacitance sensing approach has been developed to remote detect the frost porosity in real-time. An interdigital electrode was designed and fabricated to sense the capacitance changing during the frost growth based on the fringing effect. Frost growth under the same surface temperature, air temperature and relative humidity but different air velocity was observed. The averaged approach by measuring the frost mass and volume was also adopted for comparison. Result shows that the frost porosity measured by the capacitance sensing approach agrees well with the averaged measurement approach with a maximum difference of 12%. The capacitance sensing approach can measure the frost dielectric constant in good agreement with the prediction of the Maxwell-Garnett's theory as well. This approach shows great potential for real-time precise frost detection and defrost control.

1. INTRODUCTION

Frost build up on surfaces is an undesired phenomenon in many applications. As a mixture of ice and air, frost can be treated as a porous structure and frost porosity (density) is a very important parameter for understanding frost growth mechanism, frost modeling (Jones, et. al, 1975; Iragorry, et.al, 2004; Lee, et.al, 2003; Na, et.al, 2004; Hermes, et.al, 2009) and defrost control.

Frost growth is affected by the surrounding air temperature/ velocity, relative humidity, surface temperature, wettability, et. al., and the frost porosity varies as frost growing. In most scenarios, frost growing starts with the condensation and the solidification, and then one-dimensional ice crystal growth (perpendicular to the cold surface), following that is branches growing on the initial crystals and crystals growing in all directions. During the above process, the air is trapped locally in the crystals and forms a porous structure. The porosity can affect the thermal conductivity of the frost layer, and therefore the crystals growth rate, which comes back to affect the frost porosity as the feedback. As the ice crystal grows, the thermal conductivity of the frost layer decreases and eventually the temperature gradient from the cold surface to the frost-air interface is not big enough to support the crystal continuously growth, and the condensation on the interface occurs, which diffuses to the frost layer below and is solidified and the frost porosity drops. As a result, the thermal conductivity rises up and the crystals growth rate then speeds up. Therefore, the frost porosity is closely related to the stage of frost growing and strongly time dependent as frost builds up.

So far, the frost porosity (density) has been measured in most work by the mass and volume of the frost within certain accumulating period and provided as the averaged frost porosity (Shin, et. al, 2003; Sahin, et.al, 1994; Kandula, et.al, 2012), in which the time interval for the average is totally arbitrary. The measured results have big deviations and strongly affected by the operation of the measurement, which cannot explain the physics of the frost growth properly. As a mixture of ice crystal and air, frost porosity can be detected based on the dielectric constant difference between the two components using a capacitance sensor. Similar approach has been adopted to measure the percentage of components in mixtures for different applications, including void fraction (Cimorelli, et.al, 1967 and Strizzolo et.al, 1993), water fraction in crude oil (Hammer, et.al, 1989), snow porosity (Tiuri, et.al, 1984), and quartz fraction in binary mixtures (Huang, et.al, 2017), etc. However, there is no real time frost porosity detection in the open literature to our best knowledge so far.

In this work, frost porosity has been detected in real time using a self-designed and fabricated capacitance sensor. Frost growth was conducted within a wind tunnel under different conditions. The frost porosity was measured by the capacitance sensing and also using the average approach with a time interval of 5 minutes. The detection is non-intrusive and real time process and it has the dramatic effect on the understanding of frost mechanism.

2. FUNDAMENTALS OF THE FROST POROSITY MEASUREMENT USING CAPACITANCE SENSING

An interdigital electrode has been designed and fabricated for the capacitance sensing in this work (details of the electrode and the whole sensor was described in our other paper of this conference, #**272**), which is co-planer comb structure as shown in Figure 1. Unlike the parallel plate capacitor having a well-defined correlation in Eq (1), with A of the plate area in m^2, d of the distance between two plates in m and ε of the target absolute permittivity and expressed by the target dielectric constant ε_r and the electric constant ε_0 (8.854×10^{-12} F/m) as Eq (2), The capacitance sensing is based on the fringing effect and related to the electrode finger dimensions (the finger height *f*, the spacing between two fingers *s*, the fingers number *n*, and the electrode width *w*) and its structure. The capacitance reading with a target height of *l*, shown in Figure 1, can be expressed as Eq (1),

$$\mathrm{C} = b\eta^a\varepsilon_e\varepsilon_0 w \tag{1}$$

where:

b and a are constant , related to the finger configuration and determined by the calibration.

η is the electrode metallization ratio, defined as the percentage of the metal part, $\eta = f/(f+s)$.

ε_0 is the electric constant, about 8.854×10^{-12} F/m.

ε_e is the effective dielectric constant. For a 'dense' comb structure, the electric field variation along the electrodes surface can be ignored. In that case, the tested target effective area is its overlapping area with the electrodes. So, ε_e has a linear relationship with the target overlapping length if we assume target is much wider than the electrodes, as in Eq (2), in which ε_r and ε_a are the target and air dielectric constant, respectively.

$$\varepsilon_e = \frac{1}{n(f+s)}\left(\int_0^l \varepsilon_r dy + \int_l^{n(f+s)-l} \varepsilon_a dy\right) = \frac{\varepsilon_r l}{n(f+s)} + \varepsilon_a - \frac{\varepsilon_a l}{n(f+s)} \tag{2}$$

Therefore, the capacitance reading can be derived as Eq (3), where C_0 is the initial reading of the sensor without target (l=0).

$$C = b\eta^a\left(\frac{\varepsilon_r - \varepsilon_a}{n(f+s)}\right) l\varepsilon_0 w + C_0 \tag{3}$$

The target can be one pure component or a uniform mixture, and for mixture the dielectric constant ε_r is different from one sole component. According to Maxwell-Garnett's theory (Levy, et.al, 1997), for a uniform binary mixture (ice and air in this case), the dielectric constant and the volume proportion of one component hold the correlation as Eq (4),

$$\phi_1 \frac{\varepsilon_1 - \varepsilon_{12}}{\varepsilon_1 + 2\varepsilon_{12}} + (1 - \phi_1) \frac{\varepsilon_2 - \varepsilon_{12}}{\varepsilon_2 + 2\varepsilon_{12}} = 0 \tag{4}$$

where ε_1 and ε_2 is the dielectric constant of component 1 and 2, respectively, ε_{12} is the equivalent dielectric constant of the binary mixture, and ϕ_1 is the volume proportion of component 1 in the mixture, which can be then expressed as Eq (5)

$$\phi_1 = \frac{(\varepsilon_{12} - \varepsilon_2)(\varepsilon_1 + 2\varepsilon_{12})}{3\varepsilon_{12}(\varepsilon_1 - \varepsilon_2)} \tag{5}$$

With the capacitance reading, known dimension of the electrode structure, and target height, the volume proportion of component in the mixture could be obtained. In this work, the designed electrode has *w*=3mm, *n*=116, *f*=0.095mm, *s*=0.032mm, and calibrated value *a* and *b* of *a*=1.181, *b*=4.733. With all above and the measured frost thickness, we can measure the frost porosity in real time.

3. EXPERIMENTAL APPARATUS

The experiment is conducted within a wind tunnel as shown in Figure 2, in which the air flow rate, air temperature and relative humidity can be controlled to the desired condition. Frost growth on the aluminum surface of a cold plate, which connected to a chiller for surface temperature control, and the surface temperature is monitored using thermocouple installed below the surface. Electrode sensor is positioned on the side of the cold plate with a distance of 75mm to the leading edge, as shown in Figure 3, and images of the frost are also recorded by a high-speed camera. Detailed description of the experimental setup, measurement uncertainty can be referred to the other paper (Purdue Conference #**272**).

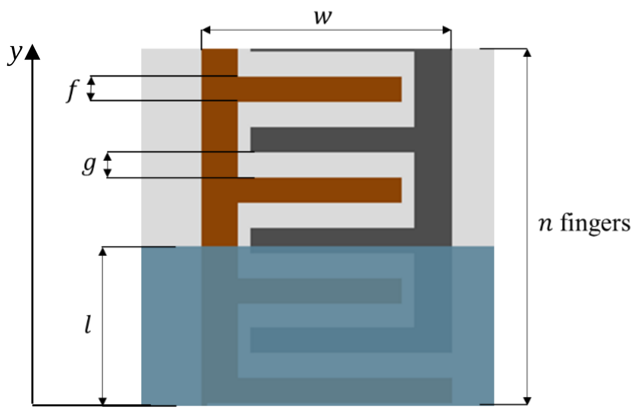

Figure 1: Interdigital electrodes with the target thickness of l

4. RESULTS AND DISCUSSION

In this work, frost growth under conditions of constant surface temperature *Ts*=-8.0 ℃ , air temperature *Ta*=13.5℃,, relative humidity RH=53% and different air velocity u_a=1.0 m/s and 3.0 m/s were observed. For comparison with the capacitance sensing, frost porosity was also measured by collecting the mass and volume of the frost. Averaging time interval for each data point is 5 minutes.

4.1 Effect of Frost Porosity on The Dielectric Constant

Frost as a mixture of air and ice crystals, the dielectric constant can be correlated to the porosity using Eq (5), with the dielectric constant of air and ice crystals of 1 and 53 (Aragones, et.al, 2010) respectively. It can be found that the frost dielectric constant decreases as the porosity increases, as shown in Figure 4. The frost dielectric constant decreases with a big slope at a small porosity (ϕ<0.6~0.7) and it decreases with a much smaller slope at the bigger porosity (ϕ>0.8). And the dielectric constant is almost linearly decreases for a small range of frost porosity within those two sections.

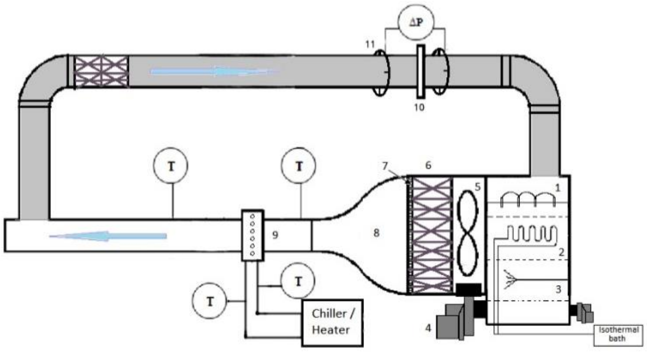

Figure 2: Schematic diagram of the wind tunnel. 1. heater; 2. cooling coil; 3. cold mist humidifier; 4. blower; 5. mixer; 6. honey comb; 7. screen; 8. contraction; 9. test section; 10. orifice plate; 11. *D* & *D*/2 pressure taps

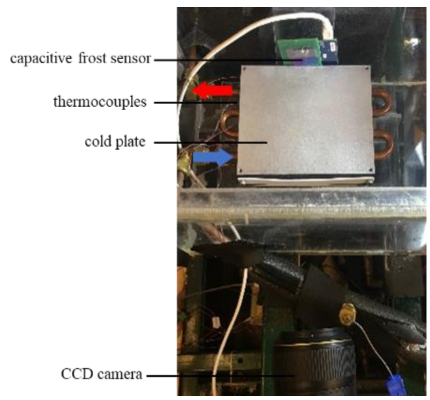

Figure 3: Test section

The dielectric constant of frost from the measurement is also shown in Figure 4 with an enlarged plot for comparison. The dielectric constant of frost decreases also linearly with the porosity shown in the experiment within a short porosity range. The measured frost dielectric constant agrees well with the prediction by Maxwell-Garnett's theory.

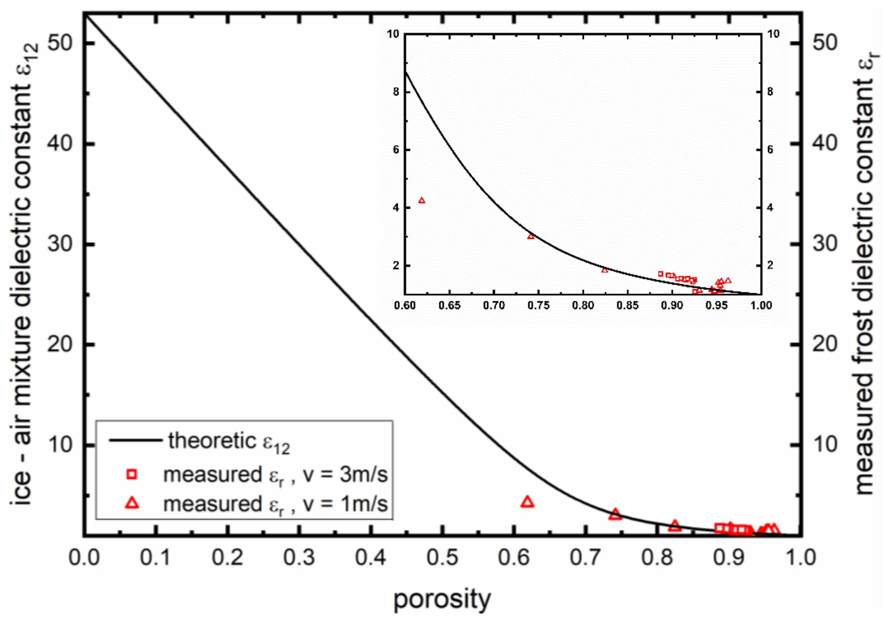

Figure 4: Frost dielectric constant versus porosity (comparison of theory and experiment results).

4.2 Frost porosity with different air velocity

Frost porosity was measured by both capacitance sensing and average approach. The average approach is measuring the frost weight every 5 minutes by collecting the defrost water, together with the thickness of frost from the image processing, the frost density (porosity) can be obtained by the mass and the volume. Result from both approaches is shown in Figure 5(a) and (b) under air velocity of 1.0 m/s and 3.0 m/s respectively

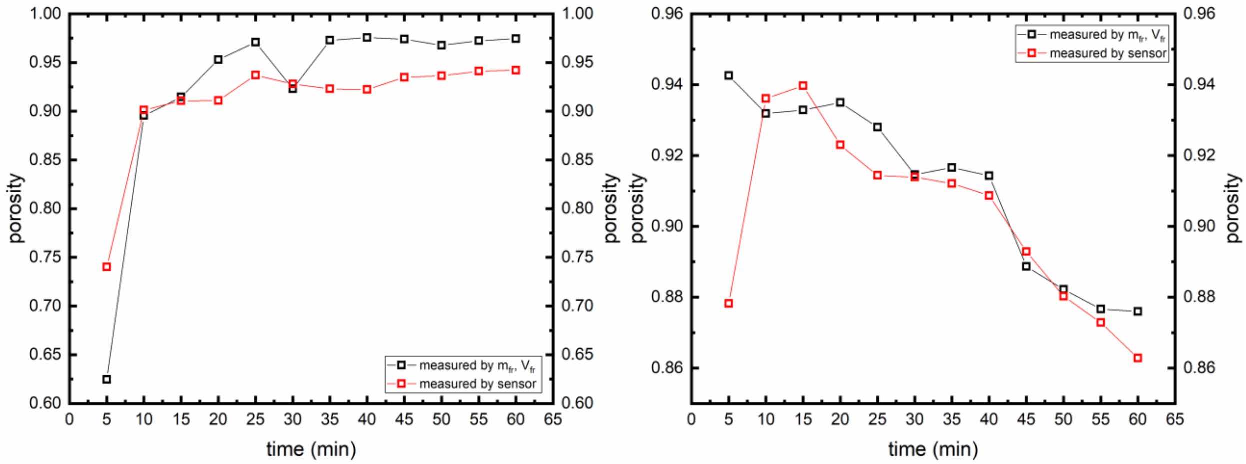

(a) Air velocity u_a=1.0 m/s (b) air velocity u_a=3.0m/s

Figure 5: Frost porosity measured with different approach with same surface temperature (-8.0 °C), same relative humidity (53%), and same air temperature (13.5 °C).

It can be found, in Figure 5(a), that the porosity of frost under air velocity of 1.0 m/s is at a low value at the beginning of the frost growth (about 0.62) and it keeps increasing for the first ~30 minutes and then it stays as a constant with a very slightly decreasing trend till 60 minutes (the end of the experiment), which has been captured well by both approaches. The porosity recorded by the capacitance sensing agrees very well with the averaged approach with a maximum difference of about 12%. The frost porosity, shown in Figure 5(b), at the air velocity of 3.0 m/s keeps decreasing, and it drops from 93% to 89% according to the averaged approach and from 97% to 85% according to the capacitance sensing approach. And the maximum difference of capacitance sensing from the averaged approach is about 5% in this test.

The porosity of frost at a low air velocity is usually higher than that at a high air velocity, which can be reflected by the test results shown above after 25 minutes for both approaches. It is especially clear by comparing the capacitance sensing results for the two cases. The general explanation for that is due to a higher frost-air interface temperature at a high air velocity, so the frost is more likely subjected to local melting and water diffuses through the frost layer. However, during the first 25 minutes, it is a different story with more complex mechanism involved. It is not very clear about the reason of the porosity behaves in the way observed.

5. CONCLUSIONS

Frost porosity measurement has been conducted in this work using a designed capacitance sensing approach. Frost growth on aluminum surface under the same surface temperature, the same air temperature and relative humidity but different air velocity was observed. An averaged frost porosity measurement approach by collecting the defrost mass and frost volume was also adopted for comparison. The results show that:

1) The frost porosity slowly decreases under the air velocity of 3.0 m/s during the whole frost growth period (60 minutes), but it increases for the first 25 minutes and then slowly decreases under the air velocity of 1.0 m/s.
2) The capacitance sensing approach agrees well with the averaged measurement approach with a maximum difference of 12%

3) The capacitance sensing approach can measure the frost dielectric constant in good agreement with the prediction of the Maxwell-Garnett's theory.

REFERENCE

Aragones, J. L., MacDowell, L. G., & Vega, C. (2010). Dielectric constant of ices and water: a lesson about water interactions. The Journal of Physical Chemistry A, 115(23), 5745-5758.

Chetpattananondh, K., Tapoanoi, T., Phukpattaranont, P., & Jindapetch, N. (2014). A self-calibration water level measurement using an interdigital capacitive sensor. Sensors and Actuators A: Physical, 209, 175-182.

Cimorelli, L., & Evangelisti, R. (1967). The application of the capacitance method for void fraction measurement in bulk boiling conditions. International Journal of Heat and Mass Transfer, 10(3), 277-288.

Farahani, H., Wagiran, R., & Hamidon, M. N. (2014). Humidity sensors principle, mechanism, and fabrication technologies: a comprehensive review. Sensors, 14(5), 7881-7939.

Hammer, E. A., Tollefsen, J., & Olsvik, K. (1989). Capacitance transducers for non-intrusive measurement of water in crude oil. Flow Measurement and instrumentation, 1(1), 51-58.

Hermes, C. J., Piucco, R. O., Barbosa Jr, J. R., & Melo, C. (2009). A study of frost growth and densification on flat surfaces. Experimental Thermal and Fluid Science, 33(2), 371-379.

Huang, J., Lu, Y., & Wang, H. (2017). A new quantitative measurement method for mixing and segregation of binary-mixture fluidized bed by capacitance probe. Chemical Engineering Journal, 326, 99-108.

Huang, J. Q., Li, B., & Chen, W. (2016). A CMOS MEMS humidity sensor enhanced by a capacitive coupling structure. Micromachines, 7(5), 74.

Iragorry, J., Tao, Y. X., & Jia, S. (2004). A critical review of properties and models for frost formation analysis. HVAC&R Research, 10(4), 393-420.

Jones, B. W., & Parker, J. D. (1975). Frost formation with varying environmental parameters. Journal of Heat Transfer, 97(2), 255-259.

Kandula, M. (2012). Frost growth and densification on a flat surface in laminar flow with variable humidity. International Communications in Heat and Mass Transfer, 39(8), 1030-1034.

Kitsara, M., Goustouridis, D., Chatzandroulis, S., Chatzichristidi, M., Raptis, I., Ganetsos, T., ... & Dias, C. J. (2007). Single chip interdigitated electrode capacitive chemical sensor arrays. Sensors and Actuators B: Chemical, 127(1), 186-192.

Lee, K. S., Jhee, S., & Yang, D. K. (2003). Prediction of the frost formation on a cold flat surface. International journal of heat and mass transfer, 46(20), 3789-3796.

Levy, O., & Stroud, D. (1997). Maxwell Garnett theory for mixtures of anisotropic inclusions: Application to conducting polymers. Physical Review B, 56(13), 8035.

Ma, R. H., Wang, Y. H., & Lee, C. Y. (2011). Wireless remote weather monitoring system based on MEMS technologies. Sensors, 11(3), 2715-2727.

Na, B., & Webb, R. L. (2004). New model for frost growth rate. International Journal of Heat and Mass Transfer, 47(5), 925-936.

Şahin, A. Z. (1994). An experimental study on the initiation and growth of frost formation on a horizontal plate. EXPERIMENTAL HEAT TRANSFER An International Journal, 7(2), 101-119.

Shin, J., Tikhonov, A. V., & Kim, C. (2003). Experimental study on frost structure on surfaces with different hydrophilicity: density and thermal conductivity. Journal of Heat Transfer, 125(1), 84-94.

Strizzolo, C. N., & Converti, J. (1993). Capacitance sensors for measurement of phase volume fraction in two-phase pipelines. IEEE Transactions on instrumentation and measurement, 42(3), 726-729.

Tiuri, M., Sihvola, A., Nyfors, E. G., & Hallikaiken, M. (1984). The complex dielectric constant of snow at microwave frequencies. IEEE Journal of oceanic Engineering, 9(5), 377-382.

ACKNOWLEDGEMENT

This work received financial support from the Air Conditioning and Refrigeration Center (ACRC) at the University of Illinois at Urbana-Champaign.